Synthesis and Characterization of the First Liquid Single-Source Precursors for the Deposition of Ternary Chalcopyrite ($CuInS_2$) Thin Film Materials

Kulbinder K. Banger,† Jonathan Cowen,‡ and Aloysius F. Hepp*,§

Ohio Aerospace Institute, Cleveland, Ohio 44142, Department of Chemistry, Cleveland State University, Cleveland, Ohio 44115, and Photovoltaic & Space Environments Branch, NASA Glenn Research Center, Cleveland, Ohio 44135

Received June 19, 2001
Revised Manuscript Received September 11, 2001

The fabrication of polycrystalline chalcopyrite absorber layers for thin film solar cells has received considerable interest due to the potential of these materials as the next generation of photovoltaic devices.[1] Chalcopyrite materials are highly appealing given their band gaps are near optimum for either implementation in space (AM0) or terrestrial applications (AM1.5). For example, a $Cu(In,Ga)Se_2$-based thin film solar cell has been reported to display an AM1.5 conversion of 18.8%.[2] A further challenge for space applications is the optimization of mass specific power to minimize power system launch costs. This requirement necessitates the use of lightweight substrates such as metal foils, or polymer substrates, which require the use of reduced-temperature processes, typically <400 °C. Consequently, greater demand has been placed on the synthesis of new precursors capable of producing chalcopyrite materials at reduced temperatures. Clearly, molecular engineering of MOCVD precursors plays a significant role and is receiving greater attention.[3] Ternary single-source precursors (type I−III−IV_2) provide an attractive and clean approach; however, very few are known or have been tested.

In the course of our investigations for improved precursors for the chemical vapor deposition (CVD) of chalcopyrite thin films,[4−6] we have discovered new liquid single-source precursors to the ternary semiconductor $CuInS_2$, based on the $[\{PR_3\}_2Cu(SR')_2In(SR')_2]$ architecture.[7] Manipulation of the steric and electronic properties of the neutral donor ligand and the thiol moiety permits directed adjustment of the physical and thermal properties of the precursor. Use of extended alkyl groups resident either on the phosphine or on thiol groups affords the liquid derivatives $[\{P(n\text{-}Bu)_3\}_2Cu(SEt)_2In(SEt)_2]$ (**1**) and $[\{P(n\text{-}Bu)_3\}_2Cu(S(n\text{-}Pr))_2In(S(n\text{-}Pr))_2]$ (**2**), respectively.

The complexes are synthesized based on a modification of the procedure reported by Kanatzidis,[7] with the thiol derivative being generated in situ by reaction of the conjugate acid with NaOEt in methanol, thus producing no adverse side products, in addition to an "activated" thiolate. The multistage synthesis yields the desired products in good yields (>65%), as opaque liquids that are stable in air for over 5 h, during normal handling.[8] One of the key features of these new precursors is their liquid phase, which is remarkable considering their high molecular mass and stoichiometery, thus facilitating the possibility of a solvent-free delivery and higher deposition rates during thin film fabrication. Needless to say, the precursors also display very high solubility in both polar and nonpolar organic solvents, which may be attributed to their ionic character and to the nonpolar alkyl groups resident on the phosphine.

Multinuclear NMR, low-temperature differential scanning caloriometry (DSC), and thermogravimetric analyses (TGA) with evolved gas analysis (EGA) were used to characterize and verify precursor formation and purity. NMR data demonstrated that **1** and **2** were free from any starting reagents (see Supporting Information). ^{31}P NMR spectra show a shift for PBu_3, from −32.50 to −19.2 for $[\{PBu_3\}_2Cu\{MeCN\}_2]^+PF_6^-$, −22.4 for **1** and −22.5 ppm for **2**, which is indicative of ligand to metal coordination and hence complex formation.[9] Low-temperature DSC provided information on the thermal stability and temperature-dependent phase changes of the single source precursors. The samples were heated at a rate of 10 °C/min under a dinitrogen

* To whom correspondence should be addressed.
† Ohio Aerospace Institute.
‡ Cleveland State University.
§ NASA Glenn Research Center.

(1) Basol, B. M. *Thin Solid Films* **2000**, *361*, 514. (b) Klenk, M.; Schenker, O.; Alberts, V.; Bucher, E. *Thin Solid Films* **2001**, *387*, 47. (c) Harris, D. J.; Hehemann, D. G.; Cowen, J. E.; Hepp, A. F.; Raffaelle, R. P.; Hollingsworth, J. A. *28th IEEE Photovoltaic Specialist Conference, Anchorage, Alaska, 2000*; p 563.

(2) Contreras, M.; Egaas, B.; Ramanathan K. *Prog. Photovoltaics* **1999**, *7*, 311.

(3) Schulz, S.; Gillan, E. G.; Ross, J. L.; Rogers, M.; Rogers, R. D.; Barron, A. R. *Organometallics* **1996**, *15*, 4880. (b) Jones, A. C.; O'Brien, P. *CVD of Compound Semiconductors: Precursors Syntheisis, Development & Application*; VCH Press: New York, 1997. (c) Kodas, T. T., Hampden-Smith, M. J., Eds. *The Chemistry Of Metal CVD*; Weinheim VCH: New York, 1994. (c) Rees, W. S., Ed. *CVD of Nonmetals*; Weinheim VCH: New York, 1996. (d) Krunks, M.; Mikli, V.; Bijakina, O.; Rebane, H.; Mere, A.; Varema, T.; Mellikov, E. *Thin Solid Films* **2000**, *1*, 61.

(4) Banger, K. K.; Cowen, J.; Harris, J.; MaClaron, R.; Riga, A.; Duraj, S.; Hepp, A. F. *Book of Abstracts; 222nd ACS National Meeting, Chicago, Illinois, 2001*. (b) Hollingsworth, J. A.; Hepp, A. F.; Buhro, W. E. *Chem. Vap. Deposition* **1999**, *5*, 105.

(5) Banger, K. K.; Harris, J.; Cowen, J.; Hepp, A. F. *E-MRS Spring Meeting, Symposium P: Thin Film Materials for Photovoltaics, Strasbourg, France, 2001*.

(6) Cowen, J.; Riga, A.; Hepp, A. F.; Duraj, S.; Banger, K. K.; MaClaron, R. *NATAS Conference Session: Thermal Application of Materials; NATAS Conference, St. Louis, MO, 2001*.

(7) Hirpo, W.; Dhingra, S.; Sutorik, A. C.; Kanatzidis, M. G. *J. Am. Chem. Soc.* **1993**, *115*, 1597.

(8) For **1**: ^1H NMR: 300 MHz; $CDCl_3$; δ 2.75 ppm (q, CH_3CH_2S−); δ 1.57 ppm (br m, $P(CH_2C_3H_7)_3$); δ 1.42 ppm (br m, $P(CH_2C_2H_4CH_3)_3$); δ 1.32 ppm (t, $-SCH_2CH_3$); δ 0.94 ppm (t, $P(CH_2C_2H_4CH_3)_3$). ^{13}C NMR 75 MHz; $CDCl_3$; δ 26.66 ppm ($P(CH_2C_3H_7)_3$); δ 24.88 ppm ($P(CH_2CH_2C_2H_5)_3$); δ 24.83 ppm ($P(C_2H_4CH_2CH_3)_3$); δ 23.22 ppm ($-SCH_2CH_3$); δ 20.87 ppm ($-SCH_2CH_3$); δ 13.89 ppm ($P(C_2H_4CH_2CH_3)_3$). ^{31}P NMR: 121 MHz; $CDCl_3$; δ −21.42 ppm (br s, $-Cu\{P(Bu_3)\}_2$). Complex **2** was prepared in a manner similar to **1**: ^1H NMR: 300 MHz; $CDCl_3$; δ 2.69 ppm (t, $C_2H_5CH_2S$−); δ 1.56 ppm (br m, $P(CH_2C_3H_7)_3$ overlapping with $CH_3CH_2CH_2S$−); δ 1.41 ppm (br m, $P(CH_2C_2H_4CH_3)_3$); δ 0.94 ppm (m, $CH_3CH_2CH_2S$− overlapping with $P(C_3H_6CH_3)_3$). ^{13}C NMR: 75 MHz; $CDCl_3$; δ 30.92 ppm ($CH_3CH_2CH_2S$−); δ 28.73 ppm ($CH_3CH_2CH_2S$−); δ 26.66 ppm ($P(CH_2C_3H_7)_3$); δ 24.96 ppm ($P(CH_2CH_2C_2H_5)_3$); δ 24.85 ppm ($P(C_2H_4CH_2CH_3)_3$); δ 13.91 ppm ($P(C_2H_4CH_2CH_3)_3$); δ 13.71 ppm ($CH_3CH_2CH_2S$−). ^{31}P NMR: 121 MHz; $CDCl_3$; δ −21.38 ppm (br s, $-Cu\{P(Bu_3)\}_2$).

(9) Brisdon, A. K. *Inorganic Spectroscopic Methods*; Oxford University Press: Oxford, UK, 1998.

10.1021/cm010507o CCC: $20.00
Published on Web 11/01/2001

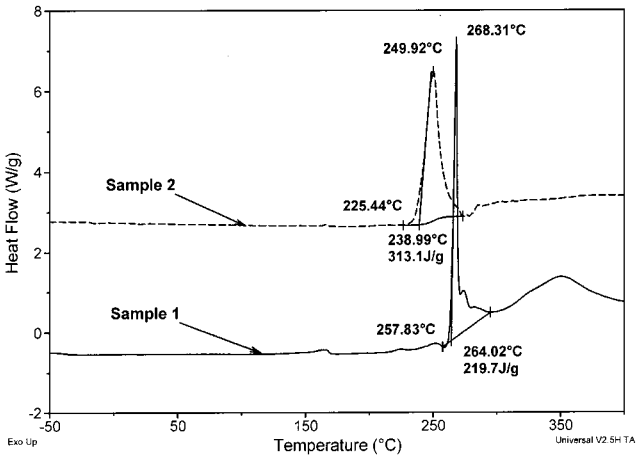

Figure 1. Low-temperature DSC Studies.

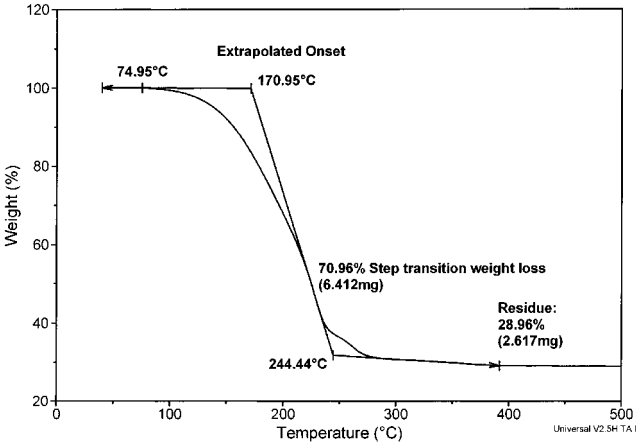

Figure 2. TGA profile for [{P(*n*-Bu)$_3$}$_2$Cu(S(*n*-Pr))$_2$In(S(*n*-Pr))$_2$], **2**.

atmosphere, using hermetically sealed aluminum pans to eliminate weight loss associated with vaporization. The low-temperature DSC profiles show an absence of an endotherm assignable to a melting phase transition, thus confirming their liquid phases at ambient temperatures (Figure 1). The main exothermic events for **1** and **2** begin with onset temperatures of 258 and 225 °C with large exotherms of 220 and 313 J/g, respectively, which can be assigned to the decomposition of the samples. The lower decomposition temperature of **2** is as expected since an increase in chain length and/or steric "bulk" of the alkyl groups is reported to decrease stability.[3c,10]

Thermogravimetric analyses (TGA) were performed at ambient pressure in platinum pans on samples of the liquid precursors. The samples were heated at a rate of 20 °C/min under a dinitrogen atmosphere to correlate with EGA. Weight loss was associated with decomposition of the complexes (Figure 2). Calculation of the derivative maximum rate of weight loss (MRW, %/°C), and step transition weight loss were used as a measure of relative stability. The TGA curves show a smooth loss of mass over a temperature window of approximately

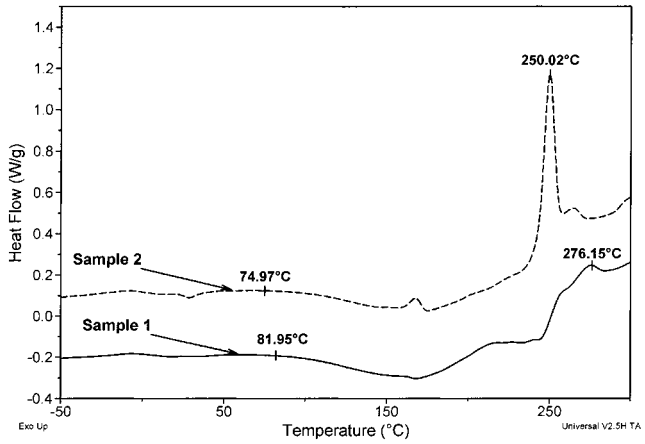

Figure 3. Low-temperature MDSC for [{P(*n*-Bu)$_3$}$_2$Cu(SEt)$_2$-In(SEt)$_2$] (**1**) and [{P(*n*-Bu)$_3$}$_2$Cu(S(*n*-Pr))$_2$In(S(*n*-Pr))$_2$] (**2**).

170 °C, accounting for a loss of 70% for **1** and 71% for **2**, of the original material where the MRW is found at 238 and 225 °C, respectively. The TGA profile for samples **1** and **2** indicate an initial weight loss, as low as 82 and 75 °C, while calculation of the extrapolated onset temperatures yields 189 and 171 °C, respectively. Calculation of the precursor efficiency for **1** and **2** to afford $CuInS_2$ as the final product shows both samples to be within 1.5% based on the residual material from the TGA experiments. Preliminary vacuum-TGA studies on **1** shows the degradation temperature window to be as low as 100−160 °C, thus making these precursors ideal candidates for use in low-temperature CVD on space-qualified substrates such as Kapton.

Interestingly, TGA data indicates that both precursors begin to decompose at much lower temperatures than that observed by DSC analysis. To resolve this issue, low-temperature modulated differential scanning caloriometry (MDSC) was undertaken, which provides information about the reversible (heat capacity) and nonreversible (kinetic) characteristics of thermal events, thereby providing greater sensitivity to deconvolute thermal phase transitions.[11] MDSC profiles for samples **1** and **2** show an onset for an endothermic phase transition occurring at ≈80 and 75 °C, respectively, which correlate with the decomposition temperatures found in TGA, while the exothermic maxima (T_{max}) are of a magnitude constant with those found in the DSC experiments (Figure 3). Hence, MDSC supports the TGA decomposition data. A more thorough interpretation of the thermal properties of these materials is presented elsewhere.[6]

The mode of decomposition for the liquid precursors **1** and **2** was investigated by FTIR and mass spectroscopic EGA. The FTIR spectra for **1** (Figure 4) show absorptions at ≈3000, 1460, 1390, 1300, and 1250 cm^{-1}, which are assignable to the initial expulsion of diethyl sulfide. Correlation with the mass spectra supports these findings on the basis of the library fit and from the assignment of the fragment and parent ions (m/z = 90). After ≈15 min the intensity of the absorptions in the IR spectra due to diethyl sulfide decrease; however, absorptions in the aliphatic regions are still evident. Comparison with the respective mass spectra allows for

(10) Welch, J. T.; Banger, K. K.; Ngo, S. C.; Claessen, R. U.; Toscano, P. J.; Eisenbraun, E. T.; Kaloyeros, A. E. *Book Of Abstracts ACS Spring 2000 National Meeting, San Francisco, USA, March 2000.* (b) Kaloyeros, A. K.; Welch, J. T.; Toscano, P. J.; Claessen, R. U.; Kornilov, A.; Banger, K. K, U.S. Patent 6099903, 2000. (c) Welch, J. T.; Toscano, P. J.; Claessen, R. U.; Kornilov, A.; Banger, K. K. International Patent WO 00/69863, 2000.

(11) Reading, M. (to TA Instruments) U.S. Patents B1 5224775, 5248199, 5335993, 5346306.

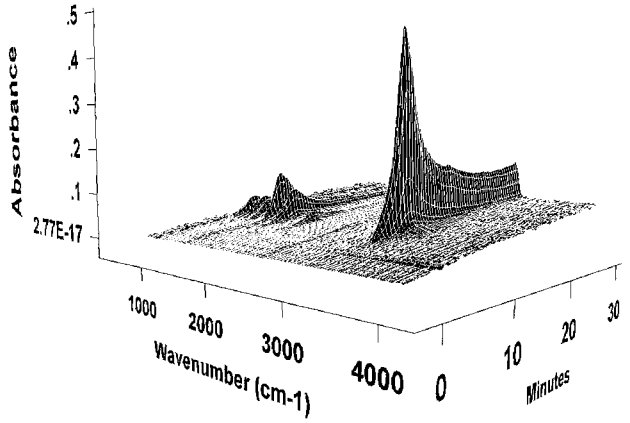

Figure 4. EGA-FTIR spectra for [{P(*n*-Bu)$_3$}$_2$Cu(SEt)$_2$In(SEt)$_2$] (**1**).

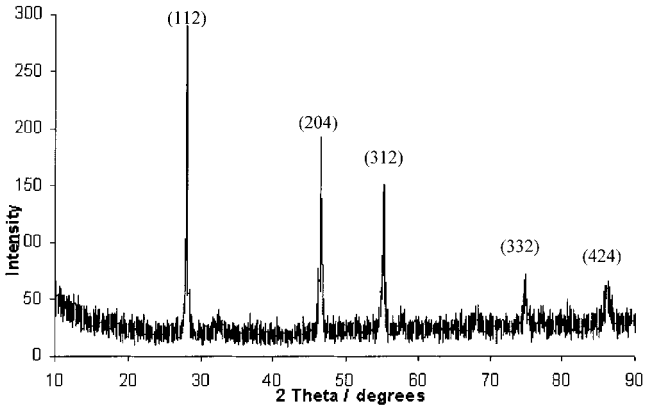

Figure 5. XRD powder diffraction for nonvolatile residue from pyrolysis of [{P(*n*-Bu)$_3$}$_2$Cu(SEt)$_2$In(SEt)$_2$] (Cu Kα, 1.541 Å).

the assignment to the loss of PBu_3, with a library fit of 92% and assignment of the parent ion (m/z = 202). Importantly, mass spectroscopic EGA shows the absence of any fragment ions with an isotopic pattern associated with an indium derivative. In a similar experiment, EGA for the *n*-propyl derivative gave analogous results.

The ability of the new precursor to thermally decompose to yield single-phase $CuInS_2$ was investigated by powder X-ray diffraction (XRD) analysis and energy-dispersive spectroscopy (EDS) on the nonvolatile solids from the TGA experiments and vacuum pyrolysis (5 mm Hg, 150−300 °C). XRD spectra for the nonvolatile material produced from the pyrolysis of **1** confirmed it to be single-phase $CuInS_2$ (Figure 5). Examination of the EDS spectra for the same samples shows predominant emissions due to Cu, In, and S edges, with the approximate percentage atomic composition of 27, 23, and 50 for **1** and 28, 23, and 49 for **2**, respectively, thus supporting the stoichiometric formation of $CuInS_2$, albeit slightly copper-rich.[12] The stoichiometry of CIS deposition is known to be temperature-dependent,[4b] and so these initial results are very promising.

(12) Samples were characterized by transmission spectroscopy (Perkin-Elmer, Lambda-19), scanning electron microscopy (SEM) (Hitachi S-3000N), energy-dispersive spectroscopy (EDS) (EDAX, accurate to ±3%), XRD (Philips PW3710, Cu Kα, 1.541), and thermal analysis (TA Instruments Models: Hi-Res-TGA-2950, DSC-910, and MDSC-2920).

In summary, we have produced the first known liquid single-source precursors for the deposition of the ternary chalcopyrite $CuInS_2$. Thermal analysis supports that selective adjustment of the sterically demanding groups either on the donor group or chalcognide permits adjustment of the solid-state phase and stability of the precursor. Furthermore, the availability of a liquid-phase precursor dramatically broadens the potential for a number of MOCVD processes and may allow application to certain spin-coating processes, fabrication of $CuInS_2$ quantum dots, and impregnated CIS_2 polymer films.

Acknowledgment. We thank NASA for financial support cooperative agreement NCC3-817, Daniel Scheimen, for assistance with TGA/DSC experiments, and Dr. David Hehemann, Dr. Stan Duraj, and Dr. Alan Riga for laboratory resources.

Supporting Information Available: Synthetic scheme for **1** and **2**. ^{1}H, ^{13}C, and ^{31}P NMR spectra of **1**, **2,** and starting reagents. TGA data for **1**. Vacuum TGA data for **1**. X-ray powder diffraction data for **1** and **2**. EDS data and spectra for **1** and **2**. SEM pictures of $CuInS_2$ from **1** and **2**. FTIR spectra (EGA) for **2**. Mass spectra (EGA) for **1** and **2** (PDF). This material is available free of charge via the Internet at http://pubs.acs.org.

CM010507O